Optical Microfiber-loaded surface plasmonic TE-pass polarizer

Youqiao Ma[1, *], Gerald Farrell[1], Yuliya Semenova[1], Binghui Li[1], Jinhui Yuan[3], Xinzhu Sang[3], Binbin Yan[3], Chongxiu Yu[3], Tuan Guo[4] and Qiang Wu[2, 1*]

[1] Photonics Research Center, School of Electronic and Communications Engineering, Dublin Institute of Technology, Kevin Street, Dublin 8, Ireland

[2] Department of Physics and Electrical Engineering, Northumbria University, Newcastle Upon Tyne, NE1 8ST, United Kingdom

[3] State Key Laboratory of Information Photonics and Optical Communications, Beijing University of Posts and Telecommunications, P.O. Box 72, Beijing 100876, China

[4] Institute of Photonics Technology, Jinan University, Guangzhou 510632, China

**Corresponding author: Qiang.wu@northumbria.ac.uk and mayouqiao188@hotmail.com*

Abstract: We propose a novel optical microfiber-loaded plasmonic TE-pass polarizer consisting of an optical microfiber placed on top of a silver substrate and demonstrate its performance both numerically by using the finite element method (FEM) and experimentally. The simulation results show that the loss in the fundamental TE mode is relatively low while at the same time the fundamental TM mode suffers from a large metal dissipation loss induced by excitation of the microfiber-loaded surface plasmonic mode. The microfiber was fabricated using the standard microheater brushing-tapering technique. The measured extinction ratio over the range of the C-band wavelengths is greater than 20 dB for the polarizer with a microfiber diameter of 4 μm, which agrees well with the simulation results.

Key words: Plasmonics, Fiber optics, Nanofiber, Polarizers

Introduction

Polarization state control of the light is of great interest for many photonic circuit applications, especially for systems operating with one single polarization [1]. One way to address this issue is to split light into two orthogonal polarizations utilizing a polarization beam splitter (PBS) [2-3]. While the solution involving a PBS is satisfactory it comes at a price of increased system complexity. Another approach is to use a polarizer to transit the wanted polarization state and extinguish the undesired polarization state by refection, redirection or absorption [4]. Recently a number of polarizers have been proposed, such as photonic crystal waveguides [5], silicon waveguides [6] and surface plasmon polaritons (SPPs) waveguides [7]. Among them SPPs (which originate from the strong coupling between the photons and free electrons on the metal surface) waveguides have been extensively explored over the last decade due to their remarkable capacities for overcoming the diffraction limit [8]. Basically only the TM polarized light (with an electric field perpendicular to the metal surface) can be coupled to the high-loss SPPs mode while the TE polarized light cannot, which makes SPPs ideal for constructing highly compact polarizers. Based on the principle of polarization-dependent excitation, Y. Wakabayashi proposed a TM-pass/TE-stop polarizer consisting of a silver film sandwiched between dielectric gratings and demonstrated an extinction ratio more than 17 dB over a wavelength range of 1500 nm to 1750 nm [9]. Using a side polished fiber coated with a graphene layer, Q. L. Bao proposed a TM-stop/TE-pass polarizer with an extinction ratio up to 27 dB in the telecommunications band, based on the fact that only a TE mode surface wave can be supported by the graphene layer [10]. More recently, X. Sun experimentally illustrated a hybrid plasmonic TE-pass polarizer with an extinction ratio that varies from 23 dB to 28 dB in the 1520 nm-1580 nm wavelength range, utilizing the high-loss characteristic of SPPs mode to extinguish the TM mode [11]. Although the aforementioned plasmonic polarizers show relatively high extinction ratio for the desired polarization state, they suffer from disadvantage of complex fabrication processes, or in other words, the advanced costly nanofabrication techniques are required, such as focused ion beam (FIB), electron-beam lithography (EBL), and/or reactive ion etching (RIE).

On the other hand, as a potential candidate for miniaturizing of optical components, microfibers have been attracting increasing interest due to their relatively simple fabrication process and unique properties such as surface field enhancement, strong evanescent field and subwavelength-scale dimensions [12]. Based on the microfiber structure, both active and passive devices have been proposed and demonstrated, such as lasers [13], sensors [14], resonators [15] and optical tweezers [16]. In addition the increased mode field diameter in the tapered region can result in the extinction of the fuse effect and shows significant potential for the optical network to protect the active equipment from damage caused by the fuse effect [17].

In this paper, by combining the advantages of SPPs and microfiber, a novel microfiber based plasmonic TE-pass polarizer is proposed and investigated both theoretically and experimentally. The proposed structure is based on an optical microfiber on top of a silver substrate. In this structure, the TM mode in the microfiber will be coupled to the surface plasmon mode with a portion of the energy located on the metal surface resulting in a large propagation loss. However the TE mode will not couple to the surface plasmon mode and thus most of the energy will be located in the microfiber resulting in a relatively low loss. It enables such a structure to act as a TE-pass polarizer. By using the Finite Element Method (FEM), the mode and transmission properties are studied theoretically. The numerical results indicate that an extinction ratio greater than 22 dB can be obtained with a microfiber diameter of 4 μm. Experimental investigations are also carried out with a comparison with the simulation results.

Device structure

Figure 1 (a-b) shows the schematic diagram of the proposed polarizer, which consists of a microfiber with a diameter of D directly placed on the silver layer (Ag) coated on a glass substrate with a length of L. All the structure symbols and accepted coordinate system are depicted in Fig. 1 (a-b). The modal properties and transmission of the proposed polarizer are numerically investigated by utilizing the FEM. In our numerical simulations, the wavelength dependent permittivities of SiO_2 and Ag are those defined in [18] and [19], respectively.

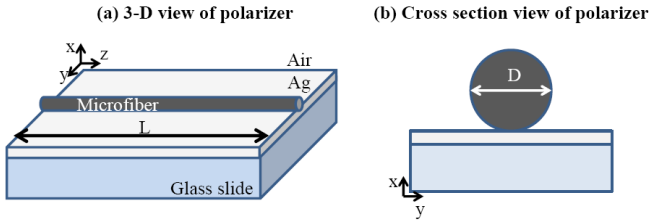

Fig.1 (a) 3-Dimentional view and (b) cross section view of the proposed polarizer. The diameter of the microfiber is *D*, and the length of the polarizer is *L*.

Simulation and design of MFLSPPs based TE-pass polarizers

It is necessary prior to an experimental investigation to carry out simulations of the proposed structures in order to underpin the design process.

Fig. 2 (a) shows the simulated wavelength dependence of the propagation length of the structure for the TM and TE modes with the microfiber diameters *D* of 3, 4 and 5 μm. This range of microfiber diameters is chosen on the basis that while fibers with diameters less than 3 μm potentially offer a better extinction ratio, fibers with diameters less than 3 μm are difficult to handle mechanically. On the other hand while large fiber diameters are easier to deal with mechanically, the extinction ratios will not be as good. Here the propagation length is calculated as

$$L_p = \lambda / [4\pi \mathrm{Im}(n_{eff})] \qquad (1)$$

where $\mathrm{Im}(n_{eff})$ is the imaginary part of the complex effective refractive index n_{eff}. As shown in Fig. 2 (a), over the wavelength range from 1500 nm to 1600 nm, the propagation length of the TE mode is much longer than that of the TM mode, or in other words, the TM mode has much higher transmission loss compared to TE mode. For example, when D = 3 μm and λ = 1550 nm, the propagation length of the TE_0 mode ($L_p(TE_0)$ = 63.6 mm) is 20.5 times longer than that of TM_0 mode ($L_p(TM_0)$ = 3.1 mm). When D = 5 μm and λ = 1550 nm, the propagation length difference between TE and TM modes becomes even larger (28.4 times longer for $L_{p(TE)}$ = 252.6 mm compared to $L_{p(TM)}$ = 8.9 mm). Based on these results, the proposed structure can be implemented as a broadband TE-pass polarizer with a flat response from 1500 to 1600 nm, by properly selecting the structure dimensions.

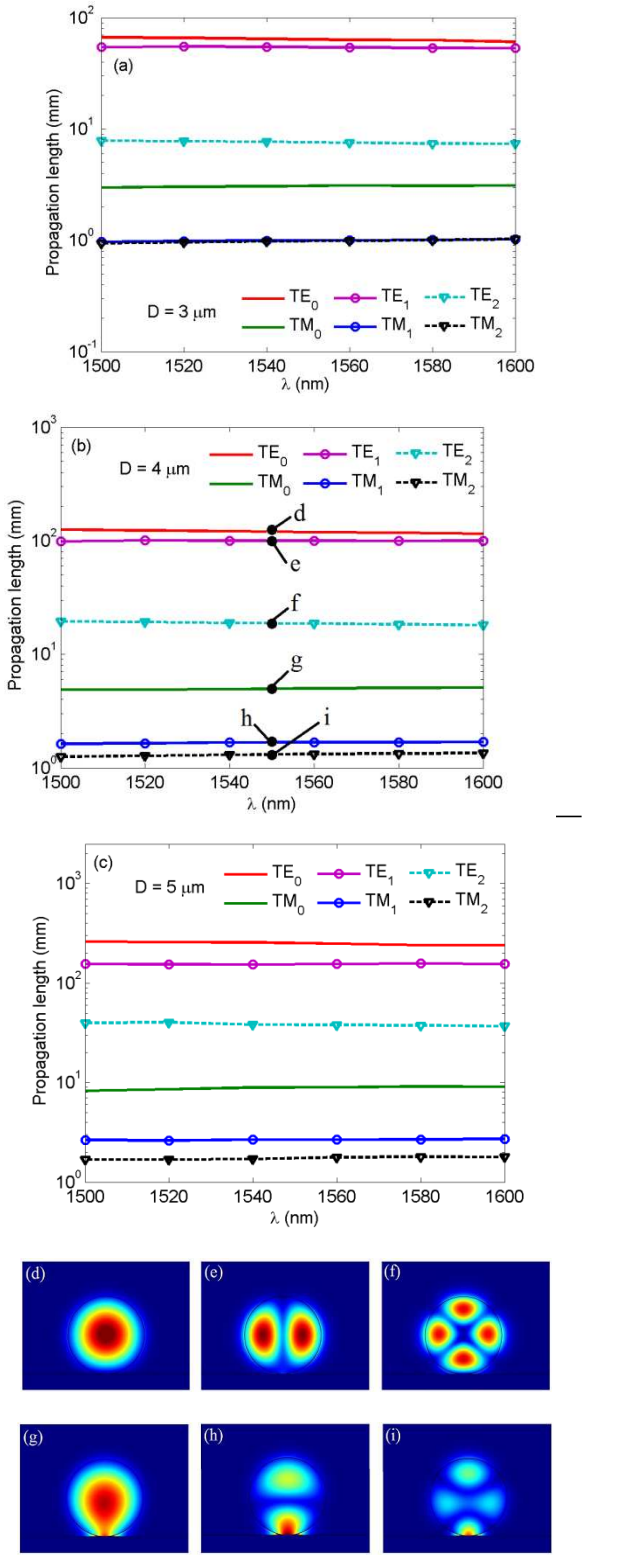

Fig.2 (a-c) Wavelength dependence of the propagation length for the microfiber with different diameter *D* for the TM and TE modes. Normalized electric energy distributions with *D* = 4 μm at the wavelength of 1550 nm: (d) TE_0 mode, (e) TE_1 mode, (f) TE_2 mode, (g) TM_0 mode, (h) TM_1 mode and (i) TM_2 mode.

To explore this loss mechanism, the normalized electric energy distributions with D = 4 μm at λ = 1550 nm corresponding to the points in Fig. 2 (b) marked as *d* (TE_0 mode), *e* (TE_1 mode), *f* (TE_2 mode), *g* (TM_0 mode), *h* (TM_1 mode) and *i* (TM_2 mode) are plotted in Figs. 2 (d), 2 (e), 2 (f), 2 (g), 2 (h) and 2 (i), respectively. From Fig. 2 (d-i), it is clear that the TE mode is confined inside the microfiber, resulting in a relatively low propagation loss. On the other hand, the TM mode is coupled to the well-known dielectric-loaded SPPs (DLSPPs) mode [20] with a portion of electric filed confined to the Ag surface, resulting in a relatively high propagation loss. Furthermore, from Fig. 2 (a) it is also found that the propagation length decreases as the diameter D decreases. The propagation length behavior could be explained by considering the percentage of evanescent field with respect to the whole field (P) which is defined as

$$P = 1 - \iint W(\vec{r})\, dS_{microfiber} / \iint W(\vec{r})\, dS_{whole} \quad (2)$$

where the electromagnetic energy density $W(\vec{r})$ is calculated as [21]

$$W(\vec{r}) = \frac{1}{2}\Re\left\{\frac{d[\omega\varepsilon(\vec{r})]}{d\omega}\right\}\left|E(\vec{r})\right|^2 + \frac{1}{2}\mu_0\left|H(\vec{r})\right|^2 \quad (3)$$

where ω is the angular frequency of the incident light, $\varepsilon(\vec{r})$ is the dielectric permittivity, μ_0 is the vacuum magnetic permeability, $\left|E(\vec{r})\right|^2$ and $\left|H(\vec{r})\right|^2$ are the intensities of electric and magnetic fields, respectively.

Fig. 3 shows the dependence of P on the diameter D at λ = 1550 nm. As shown in Fig. 3, for smaller diameters D, the evanescent field of the microfiber is stronger relative to the total field energy; hence a larger portion of power will be in contact with the metal resulting in a larger metal dissipation loss and hence shorter propagation length.

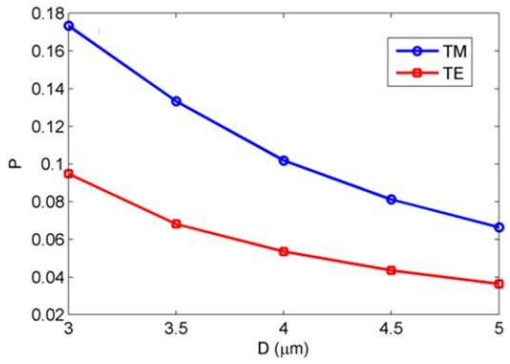

Fig. 3. The percentage of level evanescent field with respect to the level of the whole field versus the diameter D at a wavelength of 1550 nm.

The transmission of the proposed polarizer with D = 4 μm and L = 3 mm was also calculated. For this simulation, the approximate RAM requirement for the computer is larger than 500 GB due to the large ratio R between the length L of the silver substrate and simulated wavelength. Hence it was proposed to use "transfer" method as follows: the device was divided into 30 sections with the length of each section set at 100 μm. The simulation required RAM for each section was reduced to around 60 GB. The first section was calculated, and then its output boundary mode was exported as the incident boundary mode for the second section and so on. The remaining sections can be processed in the similar manner. To verify the correctness of the "transfer" method, we firstly divided a short section of 100 μm of the device into 10 sections and calculated the result and compared with calculations by simulating the 100 μm short section as a whole. It was found that both methods have the same results indicating that the "transfer" computational method is correct. Fig. 4 (a) shows the calculated transmission spectra of the TE-pass polarizer based on the "transfer" method. From Fig. 4 (a) we can find that over the range of the C-band wavelengths, the TE mode can propagate through the polarizer with a relatively low loss (insertion loss IL_{TE} < 3.8 dB) while the transmission for TM mode is suppressed (IL_{TM} > 26 dB), so that a polarization extinction ratio (ER) greater than 22 dB is achieved. Fig. 4 (b) shows IL_{TE}, IL_{TM} and ER (inset) for various microfiber diameters D at 1550 nm. As expected from Fig. 2, IL_{TE}, IL_{TM} and ER decrease as D increases. The larger extinction ratio is achieved at smaller D, but at the cost of the increased insertion loss.

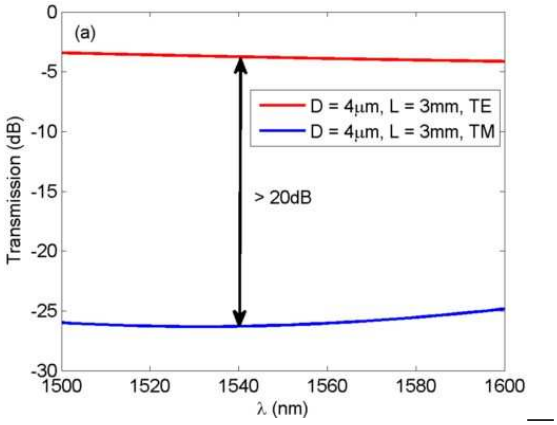

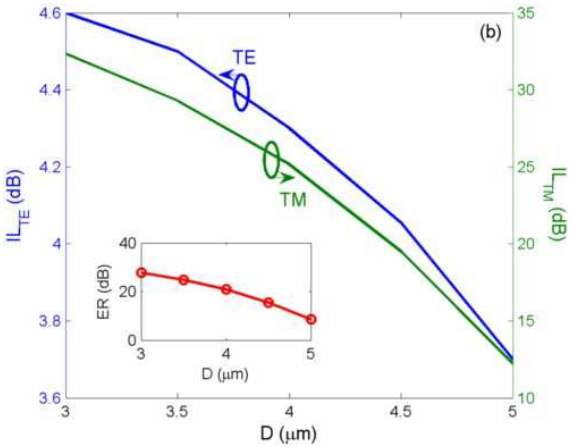

Fig.4 (a) Normalized transmission spectra for TM and TE modes. (b) Plot showing IL_{TE}, IL_{TM} and *ER* (inset) against microfiber diameter *D* at the wavelength of 1550 nm.

Experimental verification of MFLSPPs based TE-pass polarizers

To verify the theoretical analysis above, experiments were carried out for a TE-pass polarizer with microfiber dimensions of [*D*, *L*] = [4 μm, 3 mm]. The overall structure is a tapered fiber on a substrate (i.e. an Ag coated glass slide), where the length of the tapered fiber is slightly longer than that of the substrate, as shown in Fig. 1(a).

Fig. 5 shows the microfiber fabrication setup. The standard single mode fiber (SMF) SMF-28 was clamped on two linear motorized motion stages, and its middle section was heated by a ceramic micro-heater (CMH-7019, NTT-AT) to a temperature of up to 1300℃ to soften the fiber for tapering. A LabVIEW program was customized to precisely control the movement of the motion stages to control the diameter and length of the tapered microfiber.

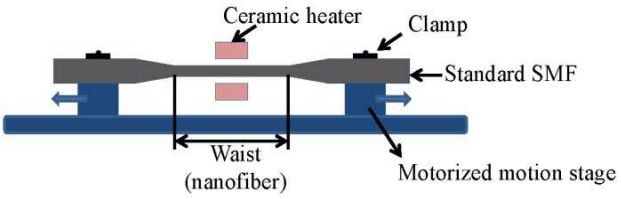

Fig.5 Optical microfiber fabrication setup.

Initially to form the substrate an Ag film with an approximate thickness of 50 nm was deposited onto a glass slide with an approximate length of 2.5 mm using a sputter coater (Q150R, Quorum), where the thickness of the Ag film was controlled by setting the deposition rate and time.

Then a tapered microfiber (i.e. with a uniform waist of 4 μm) was carefully cleaved so that it had a length slightly longer than that of the substrate, in effect there was approximately 3 mm of overhang at each end of the substrate. A tapered fiber probe was temporarily used to position the microfiber on the substrate with the aid of two 800X microscopes.

The spectral response of the TE-pass polarizer was then measured using a non-contact end-fiber coupling scheme [22]. Fig. 6 (a) and (b) show the measurement setup and a microscope image of the sample (the diameter of the microfiber is 4 μm). An end-fiber coupling scheme was used as shown in Fig 4.6 (c). Light from a broadband source was injected into a polarization controller (PC-FFB, Thorlabs), and then coupled to a tapered polarization maintaining lens ended fiber (TPMLF) (TPMJ, OZ Optics) with which had a specified focal spot diameter of 6μm. The TPMLF was then aligned to launch light to the fabricated microfiber polarizer sample. Similarly, the output light from the device was coupled into another "receiving" TPMLF, with the same specification as the launch TPMLF, the output of which was connected to an optical spectrum analyzer (OSA) (86142B, Agilent).

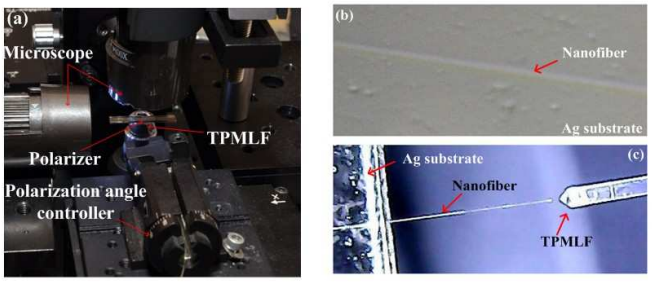

Fig.6 (a) Experiment setup for measurement of transmission. (b) Microscope image of the fabricated microfiber placed on top of an Ag substrate. (c) Microscope image of the end-fiber coupling scheme.

Before the AG substrate plus microfiber taper section structure was characterized, a low refractive index material coated substrate was used temporarily as a substitute for the Ag coated substrate, using the same microfiber to be used later with the Ag coated substrate. With this low RI substrate, a reference was established where no SPPs could exist. In the experiment, the low refractive index coated substrate was made by spin coating a polymer material (PC-363L, Luvantix) which has a low refractive index (~ 1.36 at wavelength 1550 nm) on to a glass slide.

Fig. 7 (a) shows the normalized measured spectra of the fabricated TE-pass polarizer. It can be seen that the loss of TM mode is much higher than that of the TE mode i.e. a large extinction ratio (> 20 dB) was achieved, as expected from the calculation results discussed above. By comparing results shown in Fig. 4.7 (a) and Fig. 4.4 (a), it can be found that they agree well. However the measured transmission loss is a few dB higher than the calculated results, which might be due to: 1) the scattering loss induced by roughness of the silver surface; 2) microfiber fabrication error: for example, fabrication of a microfiber with a diameter less than 4 μm could result in a larger insertion loss; 3) non-ideal microfiber's placement as shown in the inset of Fig. 4.14 (a)

resulting in the actual length of the polarizer being longer than 3 mm.

Fig. 7 (b) exhibits the measured transmission dependence versus polarization angle for the polarizer with D = 4 μm and L = 3 mm. Here we define 0° polarization as the TE mode (i.e. with an electric field parallel to the metal surface). The highest transmission is observed for 0° polarization (TE mode), and the transmission decreases gradually as the polarization angle increases. This experimental result confirms that the structure can operate successfully as a TE-pass polarizer.

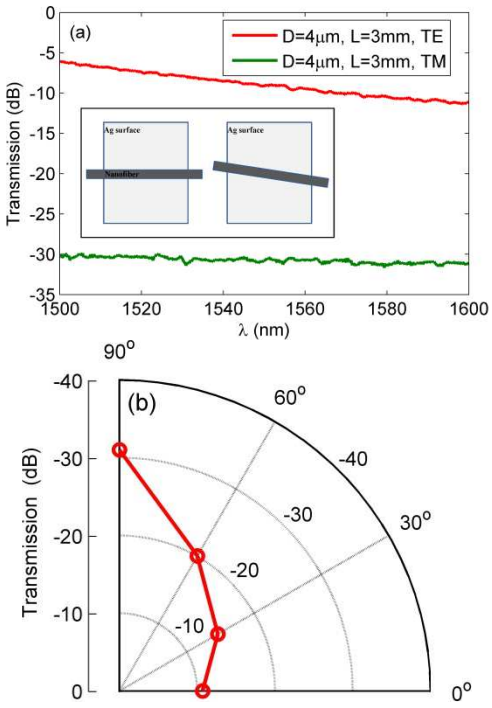

Fig.7 (a) Measured transmission spectra for TM and TE modes with dimensions of D and L. (b) Polar image of the measured transmission for different polarization angles measured at 1550 nm for D = 4 μm and L = 3 mm.

Conclusions

In conclusion, we have theoretically and experimentally demonstrated a novel surface plasmonic TE-pass polarizer which consists of an optical microfiber placed on a glass substrate coated with a 50 nm thick silver layer. Both the numerical simulation and experimental results have shown that the extinction ratio of a 3 mm-long polarizer is greater than 20 dB over the range of the C-band wavelengths.

Acknowledgements

This publication has emanated from activity supported in part by the Dublin Institute of Technology under the Fiosraigh Dean Graduate Scholarship, the Open Fund of the State Key Laboratory of Information Photonics and Optical Communications (Beijing University of Posts and Telecommunications), P. R. China and Science Foundation Ireland (SFI) under the International Strategic Cooperation Award Grant Number SFI/13/ISCA/2845.

References

[1] D. Dai, J. Bauters, and J. E. Bowers, "Passive Technologies for Future Large-Scale Photonic Integrated Circuits on Silicon: Polarization Handling, Light Non-Reciprocity, and Loss Reduction," Light Sci. Appl. 1, 1-14 (2012).
[2] Y. Q. Ma, G. Farrell, Y. Semenova, and Q. Wu, "Low loss, high extinction ratio and ultra-compact plasmonic polarization beam splitter," Photon. Technol. Lett. 26, 660-663 (2014).
[3] J. Chee, S. Y. Zhu, and G. Q. Lo, "CMOS compatible polarization splitter using hybrid plasmonic waveguide," Opt. Express 20, 25345-25355 (2012).
[4] M. N. Abbs, C. W. Cheng, Y. C. Chang, and M. H. Shih, "An omni-directional mid-infrared tunable plasmonic polarization filter," Nanotechnology 23, 444007 (2012).
[5] Y. Cui, Q. Wu, E. Schonbrun, M. Tinker, J. Lee, and W. Park, "Silicon-based 2-D slab photonic crystal TM polarizer at telecommunication wavelength," IEEE Photon. Technol. Lett. 20(8), 641–643 (2008).
[6] Q. Wang, S. T. Ho, "Ultracompact TM-pass silicon nanophotonic waveguide polarizer and design," IEEE Photon. J. 2 (1), 49-56 (2010).
[7] X. Sun, M. Z. Alam, S. J. Wagner, J. S. Aitchison, and M. Mojahedi, "Experimental demonstration of a hybrid plasmonic transverse electric pass polarizer for a silicon-on-insulator platform," Opt. Lett. 37 (23), 4814-4816 (2012).
[8] W. L. Barnes, A. Dereux, and T. W. Ebbesen, "Surface plasmon subwavelength optics," Nature 424, 824-830 (2003).
[9] Y. Wakabayashi, J. J. Yamauchi, and H. Nakano, "A TM-pass/TE-stop polarizer based on a surface plasmon resonance," Adv. Optoelectron. 2011, 867271 (2011).
[10] Q. L. Bao, H. Zhang, B. Wang, Z. H. Ni, C. H. Y. X. Lim, Y. Wang, D. Y. Tang, and K. P. Loh, "Broadband graphene polarizer," Nat. Photon. 5, 411-415 (2011).
[11] X. Sun, M. Z. Alam, S. J. Wagner, J. S. Aitchison, and M. Mojahedi, "Experimental demonstration of a hybrid plasmonic transverse electric pass polarizer for a silicon-on-insulator platform," Opt. Lett. 37, 4814-4816 (2012).
[12] X. Q. Wu, and L. M. Tong, "Optical microfibers and nanofibers," Nanophotonics 2 (5-6), 407-428 (2013).
[13] A. Sulaiman, S. W. Harun, F. Ahmad, S. F. Norizan, H. Ahmad, "Tunable laser generation with erbium-doped microfiber knot resonator," Laser Phys. 22, 588-591 (2012).
[14] J. Y. Lou, Y. P. Wang and L. M. Tong, "Microfiber optical sensors: A review," Sensors 14 (4), 5823-5844 (2014).
[15] Y. M. Jung, G. Brambilla, G. S. Murugan and D. J. Richardson, "Optical racetrack ring-resonator based on two U-bent microfibers," Appl. Phys. Lett. 98, 021109 (2011).
[16] J. D. Swaim, J. Knittel and W. P. Bowen, "Tapered nanofiber trapping of high-refractive-index nanoparticles," Appl. Phys. Lett. 103, 203111 (2013).
[17] A. M. Rocha, G. Fernandes, F. Domingues, M. Niehus,

A. N. Pinto, M. Facao, and P. S. Andre, “Halting the fuse discharge propagation using optical fiber microwires,” Opt. Express 20, 21083-21088, (2012).
[18] H. Malitson, “Interspecimen Comparison of the Refractive Index of Fused Silica,” JOSA. 55 (10), 1205-1208 (1965).
[19] E. D. Palik, “Handbook of Optical Constants of Solids,” (Academic, 1998).
[20] A. Kumar, J. Gosciniak, V. S. Volkov, S. Papaioannou, D. Kalavrouziotis, K. Vyrsokinos, J. C. Weeber, et. al., “Dielectric-loaded plasmonic waveguide components:Going practical,” Laser Photonics Rev. 6, 938-951 (2013).
[21] R.F. Oulton, V.J. Sorger, D.A. Genov, D.F.P. Pile and X. Zhang, A hybrid plasmonic waveguide for subwavelength confinement and long-range propagation. Nat. Photon. 2, 496-500 (2008).
[22]. X . Sun, M. Z. Alam, J. S. Aitchison, and M. Mojahedi, Experimnetal demonstration of a hybri plasmonic TE-pass polarizer for silicon-on-insulator platform, Opt. Lett., 37, 4814-4816 (2012).